sciendo

Polish Journal of Chemical Technology, 20, 3, 95—102, 10.2478/pjct-2018-0044

Adsorption of congo red from aqueous solutions by porous soybean curd xerogels

Zhao Zhang[1], Yanhui Li[1,2,*], Qiuju Du[1], Qi Li[1]

[1]Laboratory of Fiber Materials and Modern Textile, The Growing Base for State Key Laboratory, Qingdao University, 308 Ningxia Road, Qingdao 266071, China
[2]College of Mechanical and Electrical Engineering, Qingdao University, 308 Ningxia Road, Qingdao 266071, China
[*]Corresponding author: e-mail: liyanhui@tsinghua.org.cn

Soybean curd is a very popular food containing high-quality protein, polyunsaturated fats, vitamins, minerals and other nutrients. This study aims to prepare porous soybean curd xerogels via a vacuum freeze drying method and uses them as adsorbents to remove congo red from aqueous solutions. The morphology and functional groups of the soybean curd xerogels were characterized using scanning electron microscopy and Fourier transform infrared spectroscopy, respectively. The adsorption properties of congo red onto the soybean curd xerogels were carried out through investigating the influencing experimental parameters such as the drying method, solution pH, adsorbent dose, contact time and temperature. The results showed that the adsorption isotherm data were fitted well to the Freundlich isotherm. Adsorption kinetics of congo red onto the soybean curd followed the pseudo-second-order kinetic model. The thermodynamic parameters, such as ΔG^0, ΔH^0 and ΔS^0, were also determined.

Keywords: Soybean curd, Congo red, Adsorption, Kinetics, Thermodynamics.

INTRODUCTION

With the rapid development of industrial civilization, more and more synthetic dyes are applied to the production activities such as leather, textile, cosmetics, paper, printing, electroplating, plastic and pharmaceuticals[1]. Congo red is an anionic acid dye and has a complex chemical composition and aromatic structure. Long-term ingestion of the waste water containing congo red can destroy the human body's blood system, liver and hematopoiesis and result in health hazardous symptoms such as difficulties in breathing, diarrhoea, vomiting and nausea[2]. On the other hand, the effluents containing congo red can change the water color and odor and cause direct damage to aquatic communities[3]. So seeking for effective method to remove excessive congo red from water has always been the goal of the scientists.

In recent years, many methods including photo-catalytic degradation[4], biodegradation[5], filtration[6] and adsorption[7] have been applied in dye removal[8]. As far as these methods are concerned, adsorption is widely considered as one of the most attractive approaches due to its high efficiency, easy operation and low cost[9]. Commonly used adsorbents such as activated carbon[10], alumina[11], silica[12], zeolite[13], new types of nanomaterials such as carbon nanotubes, graphene oxide[14], graphene[15], $MgFe_2O_4$ nanoparticles[16], MgO nanostructure[17], TiO_2 nanostructure[18], the composites like agar/graphene oxide[19], polyvinyl alcohol/graphene oxide[20], cellulose/graphene oxide[21], graphene oxide/chitosan[22] have been developed and applied in dye removal. In recent years, bioadsorbents have also been the research hotspot in field of adsorption and wastewater treatment because they are abundant, nontoxic, biodegradable and have a large number of functional groups such as amino, hydroxyl, carboxyl and sulphate[23]. Soybean curd is a popular food in East and Southeast Asian countries[24] due to its highly nutritious compositions such as protein, carbohydrates, fats, vitamins, minerals and amino acids. The formation of soybean curd is mainly attributed to the denaturation of soybean protein. The soybean protein are classified into 2S, 7S, 11S, and 15S fractions according to molecular weight and sedimentation coefficient[25]. Among them, 7S (b-conglycinin) and 11S (glycinin) are the two primary globular proteins, whose amount reaches up to 37% and 31%, respectively[26]. The globular proteins consist of segments of polypeptides linked with electrostatic interactions, hydrophobic interactions, hydrogen bonds and disulfide bonds[27]. Once it is exposed to pH, heat, ionic potential or other factors, conformational variation of globular proteins appears through a physical/chemical process, which would finally form gel caused by the denaturation of native globular proteins[28]. Soybean curd contains a large number of protein components and a large number of functional groups which benefit for dye molecule adsorption.

In this work, the porous soybean curd xerogels (SC) was prepared thorough a vacuum freeze drying method. The adsorption properties of congo red onto SC were determined through investigating the various experimental parameters such as drying method, initial concentration, solution pH, adsorbent dose, contact time and temperature. The adsorption isotherm, kinetic and thermodynamic parameters were also evaluated through fitting to various theoretical models.

MATERIAL AND METHODS

Material

The fresh soybeans and delta-gluconolactone were purchased from the Qingdao supermarket. Congo red ($C_{32}H_{22}N_6O_6S_2Na_2$, >99% in purity) was purchased from Tianjin Chemical Reagent Manufacturing Co., Ltd., China. All other reagents were of analytical grade and purchased from Sinopharm Chemical Reagent Co., Ltd., China.

Preparation of SC

The soybeans were rinsed and soaked in deionized water at room temperature for 6 h and then they were smashed into soybean milk by a soybean milk machine.

The bean dreg was removed through filtration. The soybean milk was heated to 353 K, then, a suitable amount of delta-gluconolactone was added into the heated soybean milk. The soybean milk was solidified into blocks under the effect of the delta-gluconolactone. The blocks were wrapped to extrude the moisture under certain pressure and gelled SC was prepared. SC was pre-frozen at 255 K in a refrigerator for 12 h. Then frozen SC was dried using a freeze drying method and crushed into powders for further use. By contrast, another sample was dried by a conventional method in an oven at 343 K for 12 h.

Characterization of SC

The surface morphologies of the samples were examined by scanning electron microscope (SEM, JEOL JSM-7800F, Japan). The surface functional groups of SC were determined by Fourier transform infrared spectroscopy (FTIR, Bruker Tensor37, Germany) within the wavenumber range from 400 to 4000 cm^{-1}.

Batch adsorption experiments

Batch adsorption experiments were performed for 36 h in a temperature controlled water bath shaker (SHZ--82A, Ningbo Jiangnan Instrument Factory, China) at a temperature of 298 K using 50 mL glass conical flask with 20 mL dye solution and 25 mg adsorbent. To ensure the accuracy of the obtained data, the adsorption experiments were repeated at least three times.

The influence of the solution pH on the removal of congo red was studied by varying solution pH values from 3.0 to 12.0. The adsorbent dose and initial dye concentration were 25 mg and 40 mg/L, respectively.

The effect of adsorbent dose on adsorption was investigated by adding different quantity of SC (5 to 40 mg) into 20 mL solution with initial congo red concentration of 40 mg/L. In order to observe the influence of time on adsorption, 1.25 g SC was added into 1000 mL solution with initial congo red concentration of 40 mg/L, 5 mL solution was filtrated and analyzed at predetermined time. The adsorption capacity q_t (mg/g) at time t was calculated by the following equation:

$$q_t = \left(\frac{C_0 - C_t}{m}\right) \times V \tag{1}$$

where C_0 is the initial dye concentration, C_t (mg/L) is the dye concentration at time t, m is the mass of the adsorbent (g), V is volume of the solution (L).

The temperature effect on adsorption was conducted by adding 25 mg SC into 20 mL solution with initial congo red concentrations ranging from 10 to 100 mg/L at 298 , 313 and 328 K, respectively. After adsorption equilibrium, the remaining concentration of congo red in the solution was measured using a UV-vis spectrophotometer (TU-1810, Beijing Purkinje General Instrument Co., Ltd, China) at 498 nm. The adsorption capacity of congo red onto SC at the equilibrium, q_e (mg/g) was evaluated using the following equation:

$$q_e = \left(\frac{C_0 - C_e}{m}\right) \times V \tag{2}$$

where C_e is the initial dye concentration(mg/L).

RESULTS AND DISCUSSION

Characterizations of SC

Fig. 1 shows the optical and SEM images of the oven dried and freeze dried SC. It can be seen that the color of the oven dried SC is sallow, its surface is quite glossy and compact due to shrinkage during the heating process

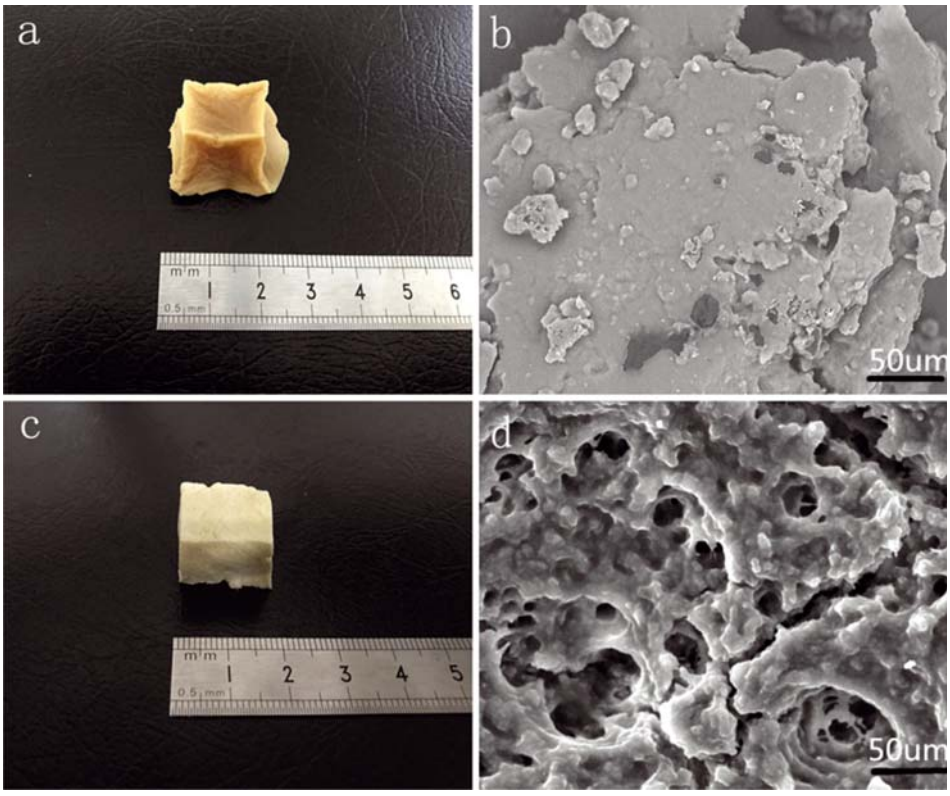

Figure 1. (a) Optical and (b) SEM image of SC made by the conventional oven drying method; (c) optical image and (d) SEM image of SC manufactured by the freeze drying method

(Fig. 1a). The SEM image (Fig. 1b) shows that the surface of the oven dried SC is very smooth and has almost no pores. The color of the freeze dried SC is milky white (Fig. 1c), its surface looks very loose and has a large number of pores (Fig. 1d). The loose structure of the freeze dried SC is attributed to special drying process of the freeze drying method. The pre-freezing treatment of SC makes the water in SC change into ice. The ice gradually sublimates under low temperature and pressure, the former position occupied by ice is left to form pore structure and there is no shrinkage of the sample, so the original morphology of SC is kept.

The FTIR spectrum of SC was characterized and shown in Fig. 2. The main broad bands are corresponding to C=O stretching vibration at 1627–1722 cm^{-1} (amide I), N–H bending at 1534 cm^{-1} (amide II) and C–N stretching vibration (amide III) at 1236 cm^{-1}, respectively[29, 30]. The band at 1055 cm^{-1} is corresponding to disulfide bond or primary alcohol absorption band. The broad band at 3278 cm^{-1} is attributed to free and bound O–H and N–H groups[31]. The band at 1158 cm^{-1} is obviously formed by a contribution of diverse groups such as out-of-plane C-H bending (from aromatic structures) and PO^{-}_{2} or P-OH stretching from phosphate esters, which are present in a large number in the protein of SC. The O-H and N-H groups in SC and O-H in adsorbed solution are certainly able to form inter- and intra-molecular hydrogen bonding with the C-O moiety of the amino acids (peptide and carboxyl groups) in the protein structure[32]. Meanwhile, the characteristic C-H stretching of CH_2 and CH_3 groups of saturated structures is found in the range 1454 cm^{-1} and 2854–2924 cm^{-1}.

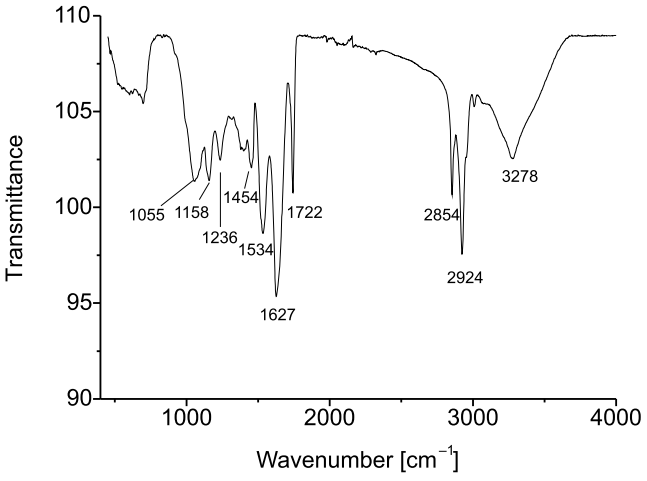

Figure 2. FTIR spectrum of SC

Congo red adsorption

Effect of drying method

To compare the effect of the drying method on the adsorption of congo red onto SC, 25 mg oven dried and freeze dried SC were put into 20 mL solution with initial congo red concentration of 40 mg/L. After equilibrium, the adsorption capacity of the oven dried SC is only 15.18 mg/g, while it increases to 27.19 mg/g for the freeze dried SC. The higher adsorption capacity of the freeze dried SC is due to its abundantly porous structures which benefit for dye molecules to diffuse into the inner cavities of SC.

Effect of solution pH

The solution pH is an important factor to affect the adsorption property of the adsorbent because it can influence the chemical properties of both dye molecule and the adsorbent. Fig. 3 shows the effect of the initial solution pH on the adsorption of congo red onto SC. It can be seen that the adsorption capacity decreases with increasing of the solution pH. Congo red is an acid-base indicator and zwitterion molecular due to the amine group ($–NH_3^+$) and sulfonated group ($–SO_3^-$)[33]. At strong acid condition, the color of congo red turns blue and the H^+ ion concentration in the solution is high. The surface of SC acquires positive charge by absorbing H^+ ions[33] and adsorbs negatively charged congo red due to sulfonated group through electrostatic attraction, which leads to a higher adsorption capacity of SC. At basic condition, the surface of SC is negatively charged by absorbing $–OH^-$ ions and can reject negatively charged congo red due to sulfonated group through electrostatic repulsion[34], resulting in a lower adsorption capacity of SC.

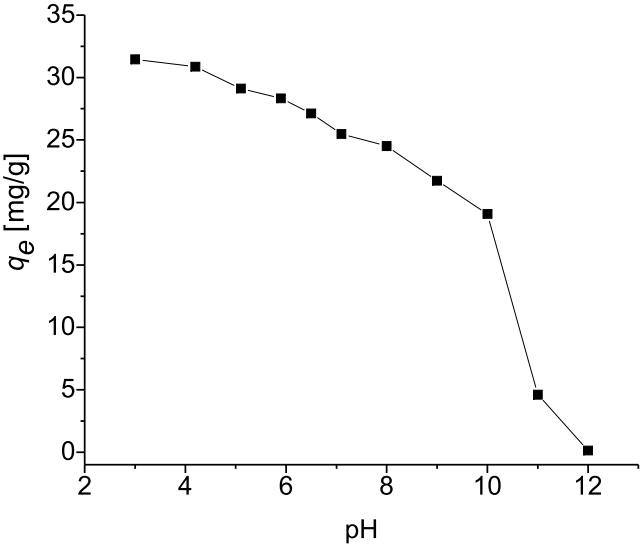

Figure 3. Effect of pH on the adsorption of congo red onto SC (initial dye concentration = 40 mg/L, dosage = 1.25 g/L, temperature = 298 K)

Effect of adsorbent dose

Fig. 4 shows the effect of adsorbent dose on the adsorption of congo red onto SC. It can be seen that the removal percentage increases with increasing the adsorbent dose, this is attributed to the increased active adsorption sites at higher adsorbent dose[35]. However, the adsorption capacity decreases with increasing the adsorbent dosage[36]. This is because that lots of effective and active sites are underused at the higher adsorbent dose. In addition, the removal percentage no longer changes significantly with further increasing the adsorbent dose as the dose reaches 25 mg. Therefore, the adsorbent dose of 25 mg was chosen in the experiments to study the influencing parameters such as pH, contact time and temperature.

Effect of contact time

Fig. 5 exhibits the relationship between adsorption capacity and contact time. It shows that at the first 200 min, the adsorption rate is very rapid, demonstrating a strong interaction existed between the congo red molecules and

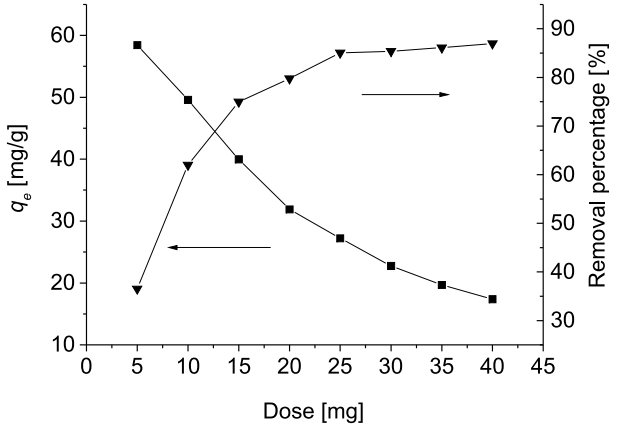

Figure 4. Effect of adsorbent dosage on the adsorption of congo red onto SC (initial dye concentration = 40 mg/L, pH = 5.8, temperature = 298 K)

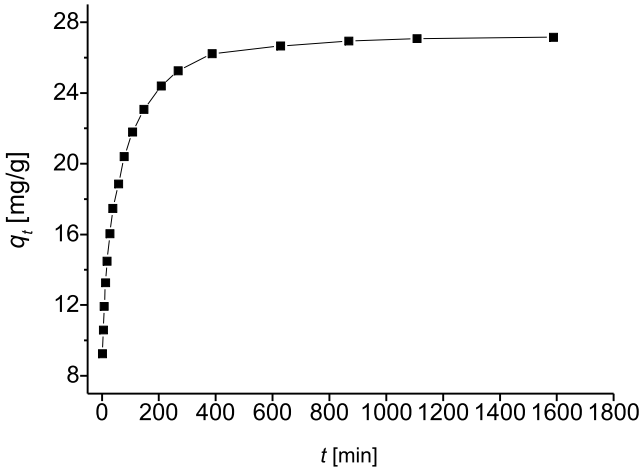

Figure 5. Effect of contact time on the adsorption of congo red onto SC (initial dye concentration = 40 mg/L, dosage = 1.25 g/L, pH = 5.8, temperature = 298 K)

the active adsorption sites on the adsorbent surface. After the initial period, the adsorption rate gradually decreases until the adsorption reaches equilibrium (about 600 min). Although the adsorption rate slows down, but the adsorption capacity is still increasing, which may be attributed to the dye molecules' extensive diffusion into the inner cavities of SC[37].

Effect of temperature

The influence of temperature on the adsorption process is shown in Fig. 6. The adsorption capacity is only 41.20 mg/g at equilibrium concentration of 10 mg/L and 298 K. It increases to 53.03 and 64.07 mg/g as the temperature rises to 313 and 328 K, indicating that the adsorption of congo red onto SC is an endothermic process.

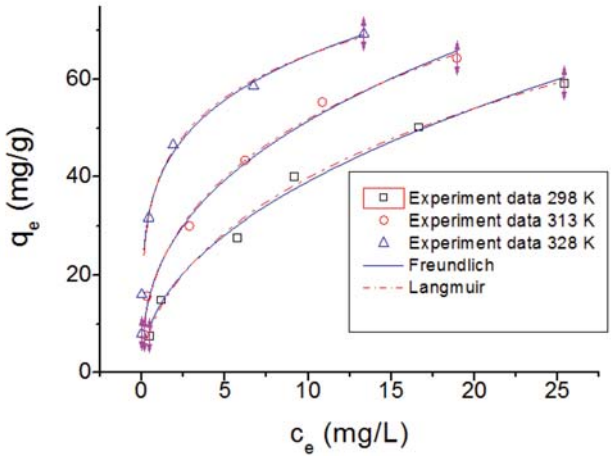

Figure 6. Adsorption isotherms of congo red onto SC (dosage = 1.25 g/L, pH = 5.8)

Adsorption isotherms

The adsorption isotherm is often used to describe the interactive behavior between the adsorbent and adsorbate[34]. The Freundlich and Langmuir models are the most frequently utilized to fit the experimental data[38]. The Langmuir model supposes that the adsorption takes place on a homogenous surface by a monolayer and equivalent sorption energies[39] and no interaction among the adsorbates on the adsorbent surface. The equation of the Langmuir isotherm is given by[40]:

$$\frac{C_e}{q_e} = \frac{C_e}{q_{\max}} + \frac{1}{q_{\max} k_L} \tag{3}$$

where $q_{\max}$ (mg/g) represents the maximum adsorption capacity, k_L (L/mg) is a Langmuir constant related to the affinity of the binding sites and energy, C_e is the equilibrium concentration of the solution (mg/L). A straight line was obtained when C_e/q_e was plotted against C_e. The values of $q_{\max}$ and k_L were calculated from the slopes and intercepts (Table 1). The maximum adsorption capacity of SC is 69.90 mg/g at 323 K. It is higher than the early reported values of various adsorbents such as CTAB--Kaolin (24.5 mg/g)[41], NiO (35.1 mg/g)[42] and Chitosan montmorillonite composite (54.5 mg/g)[43], revealing that SC is a pretty good adsorbent to remove congo red from aqueous solutions. The higher determination coefficients ($R^2 \geq 0.95489$) suggest that the adsorption of congo red onto SC follows the Langmuir model.

Besides, the Langmuir isotherm can be expressed in terms of a dimensionless equilibrium parameter R_L[44], it is defined as follows:

$$R_L = \frac{1}{1 + C_0 k_L} \tag{4}$$

Table 1. Isotherm parameters for the adsorption of congo red onto SC

T [K]	$q_{\max}$ [mg/g]	Langmuir				Freundlich			
		k_L [L/mg]	R_L	R^2	P [%]	k_F [L/mg]	n	R^2	P [%]
298	68.96	0.18	0.05–0.36	0.9549	15.466	12.36	2.00	0.9859	3.176
313	69.20	0.43	0.02–0.19	0.9651	23.766	20.21	2.44	0.9609	2.123
328	69.90	2.29	0.004–0.04	0.9876	41.164	38.87	4.46	0.9918	1.802

where C_0 is the initial concentration of congo red (10, 20, 40, 60, 80 and 100 mg/L) and k_L is the Langmuir constant (L/g).This parameter indicates the isotherm is unfavorable ($R_L > 1$), favorable ($R_L < 1$), linear ($R_L = 1$), or irreversible ($R_L = 0$). Table 1 shows that the calculated R_L values are all between 0 and 1, meaning that the adsorption of congo red onto SC is favorable[45].

The Freundlich model is assumed that the adsorption process occurs in the surface of heterogeneous medium. The equation is expressed by[46]:

$$\ln q_e = \ln k_F + \frac{1}{n} \ln C_e \tag{5}$$

where k_F is a Freundlich constant related to adsorption capacity (L/g), $1/n$ is an empirical parameter related to adsorption intensity. A straight line was obtained when $\ln q_e$ was plotted against $\ln C_e$. The values of n and k_F were calculated from the slope and intercept (Table 1). It is clear that the determination coefficient R^2 of the Freundlich model is higher than that of the Langmuir model, indicating that the Freundlich equation should be more suitable for evaluating the experimental data than Langmuir equation. The values of n in the range of 1–10 suggest that the dye is favorably adsorbed by SC. The high values of k_F indicate the high adsorption capacity and affinity of SC for congo red molecules[47].

Only the coefficient of determination is not enough to correctly assess the suitability of the mathematical model to describe the experimental data, so another better criterion for the assessment of experimental isotherm data, a parameter known as average relative error, was used to evaluate the goodness-of-fit of a model to data. The average relative error P is given by the following equation:

$$P = \frac{100}{N} \sum_{i=1}^{N} \frac{\left| q_{e,cal} - q_{e,\exp} \right|}{q_{e,\exp}} \tag{6}$$

where $q_{e,exp}$ (mg/g) is the experimental q_e at various C_e, $q_{e,cal}$ (mg/g) is the corresponding calculated q_e according to the equation under study with the best fitted parameters, and N is the number of observations. It is generally accepted that when the P value is less than 5, the fitting is considered to be excellent[48].

Table 1 shows that all the P values calculated from Freundlich model are lower than those from Langmuir model, and they are also well below the value of 5. Therefore, it can be concluded that the adsorption of congo red onto SC is better described by the Freundlich isotherm than the Langmuir model.

Kinetics studies

In order to evaluate the controlling mechanism of the adsorption process, several kinetic models including the pseudo-first-order[49], pseudo-second-order[50] and intra-particle diffusion models[51] were utilized to analyze the experimental data. The linearized-integral form of the pseudo-first-order model is described by

$$\log(q_e - q_t) = \log q_e - \frac{k_1}{2.303} t \tag{7}$$

where k_1 is the adsorption rate constant (1/min), q_e and q_t are the amounts of congo red adsorbed at equilibrium and at time t (min), respectively. The values of k_1 and q_e were calculated from the slope of the plots of $\log(q_e - q_t)$ versus t (Fig. 7a) and shown in Table 2. It can be seen that $q_{e,cal}$ (2.72 mg/g) is very far apart to the experimental data (27.15 mg/g), indicating that the adsorption of congo red onto SC is not well fitted into the pseudo-first-order kinetic model.

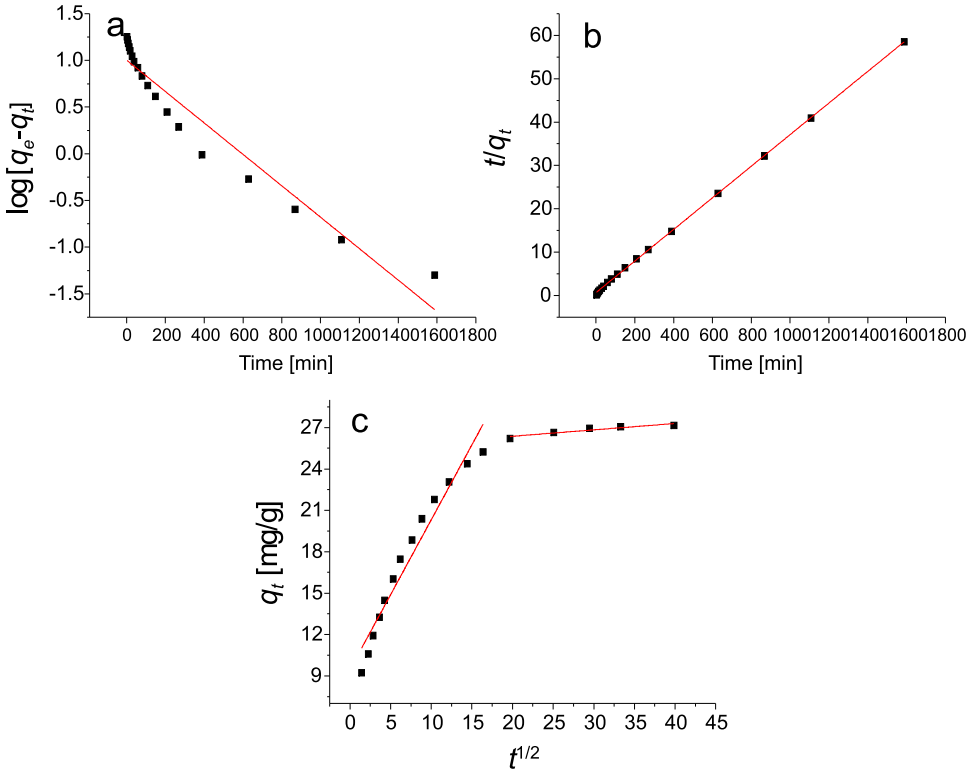

Figure 7. Adsorption kinetics of congo red onto SC: (a) pseudo-first-order; (b) pseudo-second-order and (c) intra-particle diffusion model

Table 2. Kinetic parameters for the adsorption of congo red absorbed by SC

Initial concentration [mg/L]	40	
Pseudo-first-order model	k_1 [min^{-1}]	3.87×10^{-3}
	$q_{e,exp}$ [mg/g]	27.15
	$q_{e,cal}$ [mg/g]	2.72
	R^2	0.9313
	P	41.547
Pseudo-second-order model	k_2 [g/mg min]	1.91×10^{-3}
	$q_{e,cal}$ [mg/g]	27.46
	R^2	0.9997
	P	12.018
Intraparticle diffusion model	k_{1d} [mg/g min$^{1/2}$]	1.09
	C_1 [mg/g]	9.46
	R_1^2	0.9476
	K_{1d} [mg/g min$^{1/2}$]	0.046
	C_2 [mg/g]	25.44
	R_2^2	0.8399

The linearized-integral form of the pseudo-second-order rate model is given by

$$\frac{t}{q_t} = \frac{1}{k_2 q_e^2} + \frac{t}{q_e} \tag{8}$$

where k_2 (g/(mg min)) is the rate constant of pseudo-second-order adsorption. The values of k_2 and q_e (Table 2) were calculated from the slope and intercept of straight portion of the linear plots obtained by plotting t/q_t against t (Fig. 7b). The determination coefficient of R^2 (0.9997) is very high and the calculated adsorption capacity is very close to the experimental data, demonstrating that the adsorption of congo red onto SC is well fitted into the pseudo-second-order model.

The average relative error used in the adsorption isotherm can also be applied to kinetics modelling. $q_{t,exp}$ (mg/g) is is the experimental amount of congo red adsorbed at time t (min), $q_{t,cal}$ (mg/g) is the corresponding calculated amount of congo red adsorbed at time t according to the equation under study with the best fitted parameter and the calculated q_e. The P value calculated from the pseudo-second-order model (Table 2) is much lower than that from the pseudo-first-order model. Therefore, it can be concluded that the adsorption of congo red onto SC is better described by the pseudo-second-order model than the pseudo-first-order model.

To investigate the diffusion of congo red onto SC further, the intra-particle diffusion model was employed to analyze the diffusion mechanism during the adsorption process. Generally speaking, for a porous adsorbent, the adsorption of dye molecules is regarded to follow three continuous periods. The first period is the external diffusion stage that the adsorbate molecules transport from the boundary film to the external surface of the adsorbent. In the second period, the adsorption process mainly occurs within the particles and pores of the adsorbent. The last period, which takes the longest contact time[52], demonstrates adsorption at a site on the internal surface of adsorbent.

The intra-particle diffusion model is formulated as

$$q_t = k_{id} t^{1/2} + C_i \tag{9}$$

where k_{id} is intra-particle diffusion constant (mg/g min$^{0.5}$), q_t is the quantity of adsorbed dye at time t, $t^{1/2}$ is the square root of the time and C_i is relevant to the thickness of the boundary layer. The intra-particle diffusion parameters could be calculated from the plot of q_t versus $t^{1/2}$ (Table 2).

As Fig. 7c shows, the plot is nonlinear and doesn't pass through the origin. It is a complicated course for there are two different stages during the adsorption process of congo red onto SC. The preliminary sharp step indicates that the rate of congo red removal is quick in the beginning stage which is attributed to the instantaneous availability of large surface area and numerous active adsorption sites on the external surface of SC. The second subdued portion is the gradual adsorption stage, for which it takes a long time for dye molecules to diffuse in the micropores with the decrease of dye concentration gradient, thus resulting in a low removal rate in this rate-controlled stage[53].

Thermodynamics studies

In order to accurately evaluate the effect of temperature on the adsorption process of congo red onto SC, the thermodynamic parameters such as enthalpy change (ΔH^0), entropy change (ΔS^0) and Gibbs free energy (ΔG^0) are calculated at different temperatures using the following equations:

$$\ln\left(\frac{q_e}{C_e}\right) = -\frac{\Delta H^0}{RT} + \frac{\Delta S^0}{R} \tag{10}$$

$$\Delta G^0 = \Delta H^0 - T\Delta S^0 \tag{11}$$

where R (8.314 J/(mol·K)) is the universal gas constant and T (K) is the absolute temperature in Kelvin. The values of ΔS^0 and ΔH^0 can be calculated from the intercept and the slope of the linear straight by plotting $\ln(q_e/C_e)$ versus 1/T. The values of ΔG^0 at different temperatures were calculated according to Eq. (11).

The calculated values of ΔG^0 are –3.40, –7.24 and –11.09 kJ/mol at 298, 313 and 328 K, respectively. The negative values of ΔG^0 suggest that the adsorption is a spontaneous and feasible process. The positive value of ΔH^0 (72.94 kJ/mol) indicates that the adsorption process is endothermic. The positive value of ΔS^0 (256.18 J/mol·K) manifests that at the solid-solute interface, the increase of adsorption is random.

CONCLUSIONS

The porous SC was prepared through a simple freeze drying technique. The SEM image shows that there are a large number of inner cavities in the absorbent. The result of FTIR analysis demonstrates that SC is abundant in functional groups such as hydroxyl, carbonyl and carboxyl groups. The experimental factors influencing the adsorption such as drying method, solution pH, adsorbent dosage, contact time and temperature were investigated in detail. The equilibrium data was best fitted to the Freundlich isotherm equation. The kinetic experimental data correlated well with the second-order kinetic model. The thermodynamic parameters indicated that the adsorption of congo red onto SC was an endothermic and spontaneous process.

ACKNOWLEDGEMENTS

This work was supported by the National Natural Science Foundation of China (51672140), Natural Science Foundation of Shandong Province (ZR2015EM038), Taishan Scholar Program of Shandong Province (201511029).

LITERATURE CITED

1. Parida, K.M., Sahu, S., Reddy, K.H. & Sahoo, P.C. (2011). A Kinetic, Thermodynamic, and Mechanistic Approach toward Adsorption of Methylene Blue over Water-Washed Manganese Nodule Leached Residues. *Ind. Eng. Chem. Res*. 50, 843–848. DOI: 10.1021/ie101866a.

2. Munagapati, V.S. & Kim, D.S. (2017). Equilibrium isotherms, kinetics, and thermodynamics studies for congo red adsorption using calcium alginate beads impregnated with nano-goethite. Ecotox Environ Safe. 141, 226–234. DOI: 10.1016/j.ecoenv.2017.03.036.

3. Du, Q.J., Sun, J.K., Li, Y.H., Yang, X.X., Wang, X.H., Wang, Z.H. & Xia, L.H. (2014). Highly enhanced adsorption of congo red onto graphene oxide/chitosan fibers by wet-chemical etching off silica nanoparticles. *Chem. Eng. J.* 245, 99–106. DOI: 10.1016/j.cej.2014.02.006.

4. Chong, M.N., Jin, B., Chow, C.W.K. & Saint, C. (2010). Recent developments in photocatalytic water treatment technology: *A review. Water Res.* 44, 2997–3027. DOI: 10.1016/j.watres.2010.02.039.

5. Saitoh, T., Yamaguchi, M. & Hiraide, M. (2011). Surfactant-coated aluminum hydroxide for the rapid removal and biodegradation of hydrophobic organic pollutants in water. *Water Res*. 45, 1879–1889. DOI: 10.1016/j.watres.2010.12.009.

6. Chen, L., Moon, J.H., Ma, X.X., Zhang, L., Chen, Q., Chen, L.N., Peng, R.Q., Si, P.C., Feng, J.K., Li, Y.H., Lou, J. & Ci, L.J. (2018). High performance graphene oxide nanofiltration membrane prepared by electrospraying for wastewater purification. Carbon. 130, 487–494. DOI: 10.1016/j.carbon.2018.01.062.

7. Apul, O.G. & Karanfil, T. (2015). Adsorption of synthetic organic contaminants by carbon nanotubes: A critical review. *Water Research*. 68, 34–55. DOI: 10.1016/j.watres.2014.09.032.

8. Zhuang, Y., Yu, F., Chen, J.H. & Ma, J. (2016). Batch and column adsorption of methylene blue by graphene/alginate nanocomposite: Comparison of single-network and double--network hydrogels. *J. Environ. Chem. Eng.* 4, 147–156. DOI: 10.1016/j.jece.2015.11.014.

9. Chowdhury, S. & Balasubramanian, R. (2014). Recent advances in the use of graphene-family nanoadsorbents for removal of toxic pollutants from wastewater. *Adv. Colloid Interfac.* 204, 35–56. DOI: 10.1016/j.cis.2013.12.005.

10. Yu, M., Li, J. & Wang, L.J. (2017). KOH-activated carbon aerogels derived from sodium carboxymethyl cellulose for high-performance supercapacitors and dye adsorption. *Chem. Eng. J.* 310, 300–306. DOI: 10.1016/j.cej.2016.10.121.

11. Pham, T.D., Kobayashi, M. & Adachi, Y. (2015). Adsorption characteristics of anionic azo dye onto large alpha--alumina beads. *Colloid Polym. Sci.* 293, 1877–1886. DOI: 10.1007/s00396-015-3576-x.

12. Han, H.K., Wei, W., Jiang, Z.F., Lu, J.W., Zhu, J.J. & Xie, J.M. (2016). Removal of cationic dyes from aqueous solution by adsorption onto hydrophobic/hydrophilic silica aerogel. *Colloid Surface A*. 509, 539–549. DOI: 10.1016/j.colsurfa.2016.09.056.

13. Aysan, H., Edebali, S., Ozdemir, C., Karakaya, M.C. & Karakaya, N. (2016). Use of chabazite, a naturally abundant zeolite, for the investigation of the adsorption kinetics and mechanism of methylene blue dye. Micropor Mesopor Mat. 235, 78–86. DOI:10.1016/j.micromeso.2016.08.007.

14. Wang, Y.G., Hu, L.H., Zhang, G.Y., Yan, T., Yan, L.G., Wei, Q. & Du, B. (2017). Removal of Pb(II) and methylene blue from aqueous solution by magnetic hydroxyapatite-immobilized oxidized multi-walled carbon nanotubes. *J. Colloid Interf. Sci.* 494, 380–388. DOI: 10.1016/j.jcis.2017.01.105.

15. Liu, T.H., Li, Y.H., Du, Q.J., Sun, J.K., Jiao, Y.Q., Yang, G.M., Wang, Z.H., Xia, Y.Z., Zhang, W., Wang, K.L., Zhu, H.W. & Wu, D.H. (2012). Adsorption of methylene blue from aqueous solution by graphene. Colloid Surface B. 90, 197–203. DOI: 10.1016/j.colsurfb.2011.10.019.

16. He, A.L., Lu, R.Z., Wang, Y.Y., Xiang, J., Li, Y.L. & He, D.W. (2017). Adsorption Characteristic of Congo Red Onto Magnetic MgFe2O4 Nanoparticles Prepared via the Solution Combustion and Gel Calcination Process. *J. Nanosci. Nanotech*. 17, 3967–3974. DOI:10.1166/jnn.2017.13091.

17. Nassar, M.Y., Mohamed, T.Y., Ahmed, I.S. & Samir, I. (2017). MgO nanostructure via a sol-gel combustion synthesis method using different fuels: An efficient nano-adsorbent for the removal of some anionic textile dyes. J Mol Liq. 225: 730–740. DOI: 10.1016/j.molliq.2016.10.135.

18. Nassar, M.Y., Ali, E.I. & Zakaria, E.S. (2017). Tunable auto-combustion preparation of TiO2 nanostructures as efficient adsorbents for the removal of an anionic textile dye. Rsc. Adv. 7, 8034–8050. DOI: 10.1039/c6ra27924d.

19. Chen, L., Li, Y.H., Du, Q.J., Wang, Z.H., Xia, Y.Z., Yedinak, E., Lou, J. & Ci, L.J. (2017). High performance agar/graphene oxide composite aerogel for methylene blue removal. Carbohyd Polym. 155, 345–353. DOI: 10.1016/j.carbpol.2016.08.047.

20. Yang, X.X., Li, Y.H., Du, Q.J., Wang, X.H., Hu, S., Chen, L., Wang, Z.H., Xia, Y.Z. & Xia, L.H. (2016). Adsorption of Methylene Blue from Aqueous Solutions by Polyvinyl Alcohol/Graphene Oxide Composites. *J. Nanosci. Nanotech*. 16, 1775–1782. DOI: 10.1166/jnn.2016.10708.

21. Chen, L., Li, Y.H., Hu, S., Sun, J.K., Du, Q.J., Yang, X.X., Ji, Q., Wang, Z.H., Wang, D.C. & Xia, Y.Z. (2016). Removal of methylene blue from water by cellulose/graphene oxide fibres. *J. Exp. Nanosci*. 11, 1156–1170. DOI: 10.1080/17458080.2016.1198499.

22. Li, Y.H., Sun, J.K., Du, Q.J., Zhang, L.H., Yang, X.X., Wu, S.L., Xia, Y.Z., Wang, Z.H., Xia, L.H. & Cao, A.Y. (2014). Mechanical and dye adsorption properties of graphene oxide/chitosan composite fibers prepared by wet spinning. Carbohyd Polym. 102, 755–761. DOI:10.1016/j.carbpol.2013.10.094.

23. Li, Y.H., Du, Q.J., Liu, T.H., Qi, Y., Zhang, P., Wang, Z.H. & Xia, Y.Z. (2011). Preparation of activated carbon from Enteromorpha prolifera and its use on cationic red X-GRL removal. *Appl Surf Sci*. 257, 10621–10627. DOI: 10.1016/j.apsusc.2011.07.060.

24. Rui, X., Xing, G.L., Zhang, Q.Q., Zare, F., Li, W. & Dong, M.S. (2016). Protein bioaccessibility of soymilk and soymilk curd prepared with two Lactobacillus plantarum strains as assessed by in vitro gastrointestinal digestion. *Innov Food Sci. Emerg.* 38, 155–159. DOI: 10.1016/j.ifset.2016.09.029.

25. Kumar, R., Liu, D. & Zhang, L. (2008). Advances in proteinous biomaterials. *J. Biobased Mater. Bio*. 2: 1–24. DOI: 10.1166/jbmb.2008.204.

26. Liu, D.G., Tian, H.F., Kumar, R. & Zhang, L.N. (2009). Self-Assembly of Nano Hydroxyapatite or Aragonite Induced by Molecular Recognition to Soy Globulin 7S or 11S. *Macromol. Rapid Comm.* 30, 1498–1503. DOI: 10.1002/marc.200900265.

27. Liu, D.G., Chen, H.H., Chang, P.R., Wu, Q.L., Li, K.F. & Guan, L.T. (2010). Biomimetic soy protein nanocomposites with calcium carbonate crystalline arrays for use as wood adhesive. *Bioresource Technol.* 101, 6235–6241. DOI: 10.1016/j.biortech.2010.02.107.

28. Liu, D.G., Li, Z.H., Li, W., Zhong, Z.R., Xu, J.Q., Ren, J.J. & Ma, Z.S. (2013). Adsorption Behavior of Heavy Metal Ions from Aqueous Solution by Soy Protein Hollow Microspheres. *Ind. Engin. Chem. Res*. 52, 11036–11044. DOI: 10.1021/ie401092f.

29. Lodha, P. & Netravali, A.N. (2005). Thermal and mechanical properties of environment-friendly 'green' plastics

from stearic acid modified-soy protein isolate. Ind. Crop Prod. 21,49–64. DOI: 10.1016/j.indcrop.2003.12.006.

30. Subirade, M., Kelly, I., Gueguen, J. & Pezolet, M. (1998). Molecular basis of film formation from a soybean protein: comparison between the conformation of glycinin in aqueous solution and in films. *Int. J. Biol. Macromol*. 23, 241–249. DOI: 10.1016/S0141-8130(98)00052-X.

31. Karnnet, S., Potiyaraj, P. & Pimpan, V. (2005). Preparation and properties of biodegradable stearic acid-modified gelatin films. Polym Degrad Stabil. 90, 106–110. DOI: 10.1016/j.polymdegradstab.2005.02.016.

32. Schmidt, V., Giacomelli, C. & Soldi, V. (2005). Thermal stability of films formed by soy protein isolate-sodium dodecyl sulfate. Polym Degrad Stabil. 87, 25–31. DOI: 10.1016/j.polymdegradstab.2004.07.003.

33. Lin, J.X., Zhan, S.L., Fang, M.H., Qian, X.Q. & Yang, H. *J. Environ. Manage*. 87, 193 (2008).

34. Chen, L., Li, Y., Chen, L., Li, N., Dong, C., Chen, Q., Liu, B., Ai, Q., Si, P. & Feng, J. (2018). A large-area free-standing graphene oxide multilayer membrane with high stability for nanofiltration applications. Chem. Eng. J. 345, 536–544. DOI: 10.1016/j.cej.2018.03.136.

35. El Qada, E.N., Allen, S.J. & Walker, G.M. (2006). Adsorption of basic dyes onto activated carbon using microcolumns. *Ind. Eng. Chem. Res.* 45, 6044–6049. DOI: 10.1021/ie060289e.

36. Gupta, V.K., Jain, R., Siddiqui, M.N., Saleh, T.A., Agarwal, S., Malati, S. & Pathak, D. (2010). Equilibrium and Thermodynamic Studies on the Adsorption of the Dye Rhodamine-B onto Mustard Cake and Activated Carbon. J. *Chem. Eng. Data.* 55, 5225–5229. DOI: 10.1021/je1007857.

37. Hu, Q.H., Qiao, S.Z., Haghseresht, F., Wilson, M.A. & Lu, G.Q. (2006). Adsorption study for removal of basic red dye using bentonite. *Ind. Eng. Chem. Res.* 45, 733–738. DOI: 10.1021/ie050889y.

38. Sharma, Y.C., Uma, Sinha, A.S.K. & Upadhyay, S.N. (2010). Characterization and Adsorption Studies of Cocos nucifera L. Activated Carbon for the Removal of Methylene Blue from Aqueous Solutions. *J. Chem. Eng. Data.* 55, 2662–2667. DOI: 10.1021/je900937f.

39. Into, T., Okada, K., Inoue, N., Yasuda, M. & Shibata, K. (2002). Extracellular ATP regulates cell death of lymphocytes and monocytes induced by membrane-bound lipoproteins of Mycoplasma fermentans and Mycoplasma salivarium. *Microbiol. Immunol.* 46, 667–675. DOI: 10.1111/j.1348-0421.2002.tb02750.x.

40. Langmuir, I. (1916). The constitution and fundamental properties of solids and liquids. *J. Am. Chem. Soc*. 38, 2221–2295.

41. Zenasni, M.A., Meroufel, B., Merlin, A. & George, B. (2014). Adsorption of Congo Red from Aqueous Solution Using CTAB-Kaolin from Bechar Algeria. J. Surf. Engine.Mater. Adv. Tech. 04(06): 332–341. DOI: 10.4236/jsemat.2014.46037.

42. Song, Z., Chen, L.F., Hu, J.C. & Richards, R. (2009). NiO(111) nanosheets as efficient and recyclable adsorbents for dye pollutant removal from wastewater. *Nanotechnology.* 20(27). DOI: Artn 27570710.1088/0957-4484/20/27/275707.

43. Wang, L. & Wang, A.Q. (2007). Adsorption characteristics of Congo Red onto the chitelsan/montmorillonite nanocomposite. J. Hazard. Mater. 147, 979–985. DOI: 10.1016/j.jhazmat.2007.01.145.

44. Bulut, E., Ozacar, M. & Sengil, I.A. (2008). Equilibrium and kinetic data and process design for adsorption of Congo Red onto bentonite. J. Hazard. Mat. 154: 613–622. DOI: 10.1016/j.jhazmat.2007.10.071.

45. Chen, M., Chen, Y. & Diao, G.W. (2010). Adsorption Kinetics and Thermodynamics of Methylene Blue onto p-tert-Butyl-calix[4,6,8]arene-Bonded Silica Gel. J. Chem. Eng. Data. 55, 5109–5116. DOI: 10.1021/je1006696.

46. Freundlich, H.M.F. (1906). Over the adsorption in solution. *J. Phys. Chem*. 57, 385–471.

47. Karadag, D., Turan, M., Akgul, E., Tok, S. & Faki, A. (2007). Adsorption equilibrium and kinetics of reactive black 5 and reactive red 239 in aqueous solution onto surfactant-modified zeolite. *J. Chem. Eng. Data*. 52, 1615–1620. DOI: 10.1021/je7000057.

48. Duman, O. & Ayranci, E. (2006). Adsorption characteristics of benzaldehyde, sulphanilic acid, and p-phenolsulfonate from water, acid, or base solutions onto activated carbon cloth. *Sep. Sci. Technol.* 41, 3673–3692. DOI: 10.1080/01496390600915072.

49. Lagergren, S. (1898) About the theory of so called adsorption of soluble substances. Kungliga Svenska Vetenskapsakademiens Handlingar. 24, 1–39.

50. Ho, Y.S. & Chiang, C.C. (2001). Sorption studies of acid dye by mixed sorbents. Adsorption. 7, 139–147. DOI: 10.1023/A:1011652224816.

51. Weber, W.J. & Morris, J.C. (1963). Kinetics of Adsorption on Carbon From Solution. *J. Sanit. Eng. Div*. 89, 31–60.

52. Hameed, B.H., Din, A.T.M. & Ahmad, A.L. (2007). Adsorption of methylene blue onto bamboo-based activated carbon: Kinetics and equilibrium studies. J. Hazard. Mater. 141, 819–825. DOI: 10.1016/j.jhazmat.2006.07.049.

53. Ma, J., Jia, Y.Z., Jing, Y., Yao, Y. & Sun, J.H. (2012). Kinetics and thermodynamics of methylene blue adsorption by cobalt-hectorite composite. *Dyes Pigments*. 93, 1441–1446. DOI: 10.1016/j.dyepig.2011.08.010.